

Some remarks on the kinematical and dynamical aspects of multi-valued operators

Kees Wapenaar¹
Jan Thorbecke²
Jacob Fokkema³

13A.1 Introduction

When the velocity field of the subsurface contains strong lateral variations, traveltimes of reflection and/or transmission data can become multi-valued. Migrating these data with operators that contain first arrivals only causes migration artefacts, because energy contained in later arrivals is not accounted for (Geoltrain and Brac, 1993). The most simple solution to this problem is to account only for the most energetic event. More advanced techniques employ operators based on multi-valued Green's functions [Nolan and Symes (1996), Ehinger et al. (1996), ten Kroode and Smit (1997), Van Barneveld and Verschuur (this chapter)]. Since multi-valued Green's functions account for all arrivals at the acquisition surface, they handle the amplitudes better than single-valued operators. However, it is generally overlooked that even migration operators based on multi-valued Green's functions ignore back-scattered energy (or to say it in another way, they do not compensate for transmission losses). Hence, although they improve the amplitudes of the migration output, they do not provide the final answer. In this appendix we will discuss this phenomenon in more detail and illustrate it with a numerical example. But first we review some kinematical aspects of multi-valued operators.

¹E-mail: C.P.A.Wapenaar@CTG.TUdelft.NL

²E-mail: Jant@DeMeern.SGI.com

³E-mail: J.T.Fokkema@CTG.TUdelft.NL

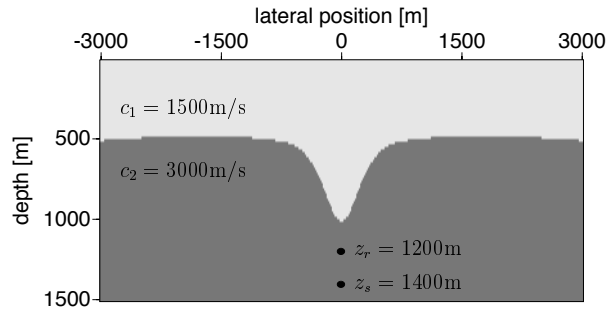


Fig. 13A.1 *Synclinal model. The response at the surface of the source at $z_s = 1400$ m will be inversely extrapolated to the indicated point at $z_r = 1200$ m.*

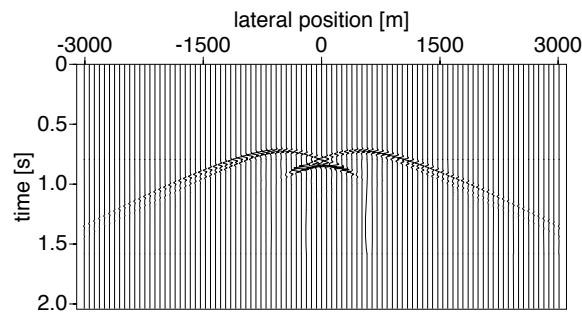


Fig. 13A.2 *The response at the surface of the source at $z_s = 1400$ m. Note the triplings. (Modeled with finite differences).*

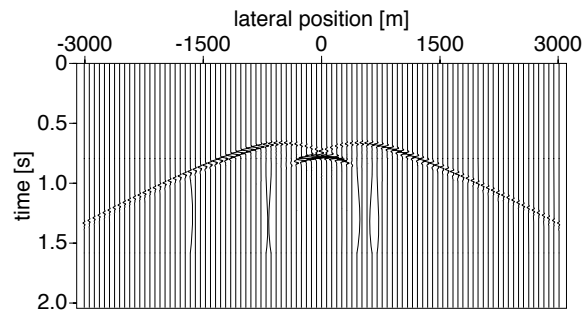


Fig. 13A.3 *The Green's wavefield at the surface (convolved with a wavelet), due to the Green's source at $z_r = 1200$ m. (Modeled with finite differences).*

13A.2 Kinematical aspects of multi-valued operators

Inverse wave field extrapolation (the nucleus of migration) may be seen as a correlation of an operator with the data. Obviously, when the operator as well as the data are single-valued,

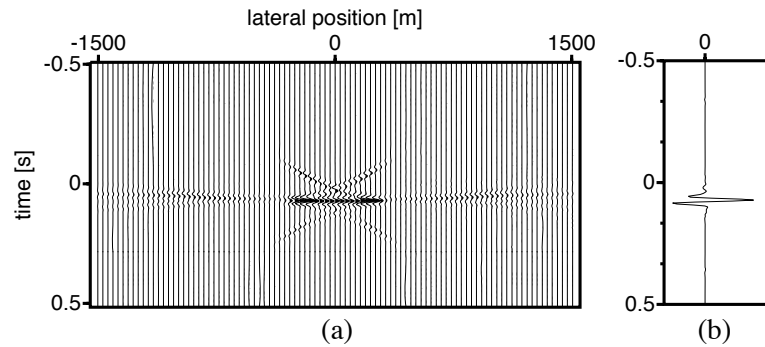


Fig. 13A.4 (a) The trace by trace correlation of Figures 13A.2 and 13A.3. Note the quintuple events. (b) Sum of the traces of Figure (a). This is the inverse extrapolation result at the indicated point at $z_r = 1200$ m in Figure 13A.1.

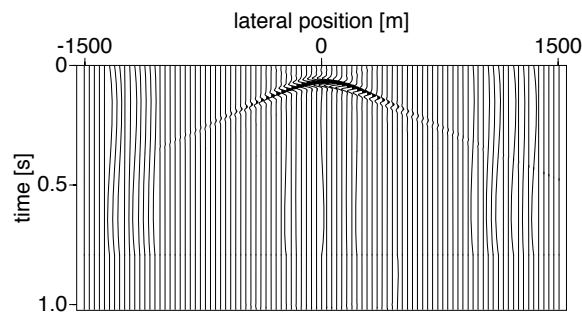


Fig. 13A.5 Inverse extrapolation result at all points at $z_r = 1200$ m. The central trace is the trace of Figure 13A.4b.

the correlation result is single-valued as well, as it should be. What is less obvious, though, is how the correlation of multi-valued data with a multi-valued operator can yield a single-valued result. This kinematical aspect is discussed in this section with the aid of a numerical example.

Consider the configuration in Figure 13A.1, which contains a synclinal structure that gives rise to triplications. Figure 13A.2 shows the response at the surface of a dipole source at $z_s = 1400$ m, vertically below the center of the aperture. For the inverse extrapolation from the surface to the indicated point at $z_r = 1200$ m we use an operator based on the Green's wavefield related to a monopole source at this point. Figure 13A.3 shows this Green's wavefield (convolved with a wavelet to get a better display). Applying the time reversed version of this operator to the data in Figure 13A.2, i.e., correlating Figures 13A.2 and 13A.3 trace by trace, one would expect *quintuples* appearing in the result. On the other hand, from the configuration in Figure 13A.1 we would expect that the inverse extrapolation result at z_r is single-valued, because the medium between z_r and z_s is homogeneous.

Figure 13A.4a shows the trace by trace correlation. Note that this result indeed contains

quintuple events. These traces have to be summed to obtain the extrapolation result at the indicated point at z_r in Figure 13A.1. The result of this summation is shown in Figure 13A.4b. The main contribution comes from the stationary event at $t = (z_s - z_r)/c_2 = 66$ ms in Figure 13A.4a; the other contributions cancel. Figure 13A.5 shows the inverse extrapolation result for all points at $z_r = 1200$ m. From this numerical inverse extrapolation example it is clear how the single-valued event is formed at the correct travel time. In the next section we will have a closer look at amplitudes.

13A.3 Dynamical aspects of multi-valued operators

To appreciate the value of using multi-valued operators, let us first repeat the experiment of the previous section with an operator that contains first arrivals only (Figure 13A.6). The results of trace by trace correlation of this operator with the data in Figure 13A.2, followed by a summation, are shown in Figures 13A.7a and 13A.7b, respectively. Note that the amplitude of the trace in Figure 13A.7b is significantly smaller than that in Figure 13A.4b, since the energy in the later arrivals in Figure 13A.2 is not accounted for. This supports the conclusion that multi-valued operators yield better amplitudes than operators containing first arrivals only.

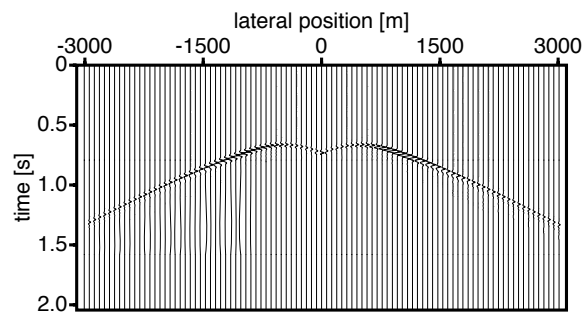


Fig. 13A.6 Operator with first arrivals only. (Obtained by muting the triplications in Figure 13A.3).

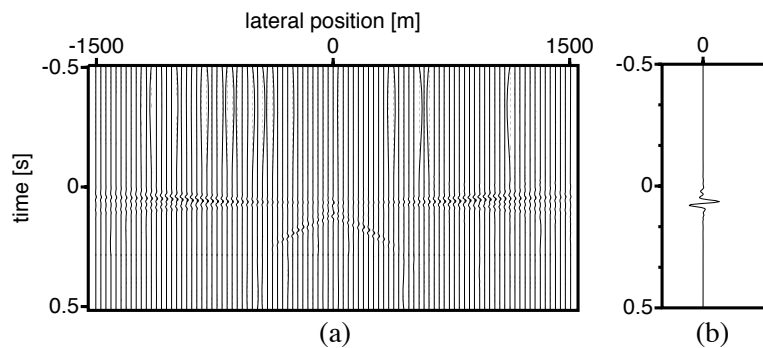


Fig. 13A.7 (a) The trace by trace correlation of Figures 13A.2 and 13A.6. (b) Sum of the traces of Figure (a).

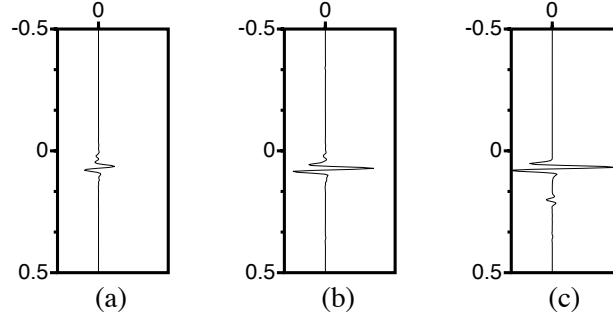


Fig. 13A.8 (a) Extrapolation result, using first arrivals only (copied from Figure 13A.7b). (b) Extrapolation result, using a multi-valued operator (copied from Figure 13A.4b). (c) The direct response at the indicated point at $z_r = 1200$ m in Figure 13A.1.

Of course we have to compare the amplitudes of both results with the desired amplitude (i.e., the amplitude of the direct response) before we can fully judge the improvement. Figure 13A.8 shows this comparison. It appears that the result of applying the single-valued operator yields an amplitude of approximately one fourth (25 %) of the correct amplitude whereas the amplitude of the result of the multi-valued operator is approximately three fourth (75 %) of the correct amplitude. Although the improvement is significant, the remaining error is significant as well. In the following we explain the cause for this error.

In order to get an exact extrapolation result at $\mathbf{x}_r = (x_r, z_r)$, one could employ the following representation integral in the space-frequency (\mathbf{x}, ω) domain [Morse and Feshbach (1953), Fokkema and Van den Berg (1993)]

$$P(\mathbf{x}_r, \omega) = \oint_S [G \nabla P - P \nabla G] \cdot \mathbf{n} dS \quad (13A.1)$$

and transform the result back to the time domain. Here S is a closed integration surface with outward pointing normal vector \mathbf{n} , P is the acoustic wavefield related to sources outside S and G is the forward propagating (or causal) Green's wavefield of a point source at \mathbf{x}_r inside S . Exploiting the time symmetry of the wave equation we may also write

$$P(\mathbf{x}_r, \omega) = \oint_S [G^* \nabla P - P \nabla G^*] \cdot \mathbf{n} dS, \quad (13A.2)$$

where G^* (the complex conjugate of G) is a backward propagating (or anti-causal) Green's wavefield [Schneider (1978), Bojarski (1983), Wapenaar and Berkhout (1989)]. Representation (13A.1) is the basis for forward and (13A.2) for inverse wavefield extrapolation; both representations are exact. The reason why in practice inverse wavefield extrapolation yields amplitude errors, despite the exactness of representation (13A.2), is because in this representation the closed surface cannot be replaced by an infinite planar surface without introducing approximations.

For the experiment of the previous section, Figure 13A.9 shows the appropriate closed surface S . The contribution of the integral in equation (13A.2) over the side surfaces vanishes when

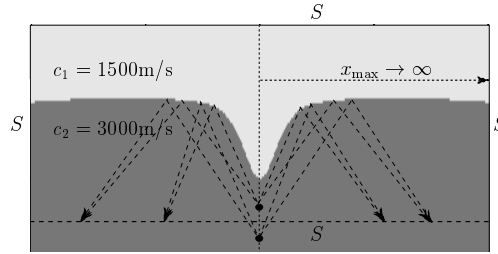


Fig. 13A.9 Closed integration surface S . The contribution of the integral (13A.2) over the lower surface (the dashed line) is ignored in the inverse extrapolation result of Figure 13A.5.

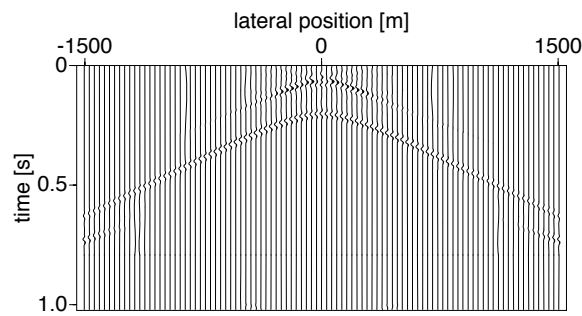


Fig. 13A.10 Contribution of the integral along the dashed line in Figure 13A.9 for all points at $z_r = 1200 \text{ m}$.

$x_{\max} \rightarrow \infty$. From Figure 13A.9 we observe that the contribution from the lower integration surface (the dashed line between \mathbf{x}_r and \mathbf{x}_s) contains, amongst others, the correlation of the *scattered* wavefield and the *scattered* Green's function. Since both these wavefields are single-valued (in this example), their correlation is also single-valued. Figure 13A.10 shows the result of the integral along the lower surface for all output points \mathbf{x}_r with $z_r = 1200 \text{ m}$. Note that this result should be added to that of Figure 13A.5 in order to obtain the full wavefield at $z_r = 1200 \text{ m}$. The first event in Figure 13A.10 is the single-valued correlation result we just discussed. It occurs at the same time as the inverse extrapolation result in Figure 13A.5; its amplitude is proportional to $R^2(\alpha)$, where $R(\alpha)$ is the angle-dependent reflection coefficient of the synclinal interface. The second event in Figure 13A.10 is the reflected downgoing wavefield at $z_r = 1200 \text{ m}$.

From this analysis we may conclude that the amplitude error, observed in Figure 13A.8, is explained by the fact that the inverse extrapolation result with the multi-valued operator lacks the contribution of the lower integration surface in Figure 13A.9.

13A.4 Conclusions

Applying operators with only first arrivals to data that contain triplications yields amplitude errors because energy contained in the later arrivals is not accounted for. The amplitudes improve when multi-valued operators are employed, since these operators account for the energy in all arrivals at the acquisition surface. However, multi-valued operators fail to account for back-scattered energy (just as single-valued operators), so they cannot fully compensate for the aforementioned amplitude errors. The amplitude errors are angle-dependent. Since they are proportional to $R^2(\alpha)$ they can be interpreted as transmission losses.

For the numerical experiment in this chapter we found that the amplitude errors when using only first arrivals are in the order of 75 %; using multi-valued operators these errors reduced to 25 %. For a further improvement, modified operators are required that account for the back-scattered energy at the lower integration surface in Figure 13A.9. Using reciprocity, the required modifications can be derived from a cross-correlation of the seismic reflection measurements at the acquisition surface (Wapenaar, 1996).

13A.5 References

- Bojarski, N. N., 1983, Generalized reaction principles and reciprocity theorems for the wave equations, and the relationship between the time-advanced and time-retarded fields: *J. Acoust. Soc. Am.*, **74**, 281–285.
- Ehinger, A., Lailly, P., and Marfurt, K. J., 1996, Green's function implementation of common-offset, wave equation migration: *Geophysics*, **61**, 1813–1821.
- Fokkema, J. T., and van den Berg, P. M., 1993, *Seismic applications of acoustic reciprocity*: Elsevier, Amsterdam.
- Geoltrain, S., and Brac, J., 1993, Can we image complex structures with first-arrival travel-time?: *Geophysics*, **58**, 564–575.
- Morse, P. M., and Feshbach, H., 1953, *Methods of theoretical physics, Vol. I*: McGraw-Hill Book Company Inc., New York.
- Nolan, C. J., and Symes, W. W., 1996, Imaging and coherency in complex structures: 66th Annual Internat. Mtg., Soc. Expl. Geophys., Expanded Abstracts, 359–362.
- Schneider, W. A., 1978, Integral formulation for migration in two and three dimensions: *Geophysics*, **43**, 49–76.
- Ten Kroode, A. P. E., and Smit, D. J., 1997, *A microlocal analysis of migration*: , SIAM, Philadelphia, Inverse problems in geophysical applications.
- Wapenaar, C. P. A., and Berkhout, A. J., 1989, *Elastic wave field extrapolation*: Elsevier Amsterdam.
- Wapenaar, C. P. A., 1996, One-way representations of seismic data: *Geoph. J. Int.*, **127**, 178–188.

Contents

13A Some remarks on the kinematical and dynamical aspects of multi-valued operators	51
13A.1Introduction	51
13A.2Kinematical aspects of multi-valued operators	52
13A.3Dynamical aspects of multi-valued operators	54
13A.4Conclusions	57
13A.5References	57